Characterization of phototransistor internal gain in metamorphic high-electron-mobility transistors

Hyo-Soon Kang, Chang-Soon Choi, and Woo-Young Choi[a)]
Department of Electrical and Electronic Engineering, Yonsei University, 134, Shinchon-dong, Seodaemoon-gu, Seoul 120-749, Korea

Dae-Hyun Kim and Kwang-Seok Seo
School of Electrical Engineering, Seoul National University, San 56-1, Sillim-dong, Gwanak-gu, Seoul 151-742, Korea

(Received 12 January 2004; accepted 16 March 2004; published online 29 April 2004)

We characterize the phototransistor internal gain of metamorphic high-electron-mobility transistors (mHEMTs). When the mHEMT operates as a phototransistor, it has internal gain provided by the photovoltaic effect. To determine this internal gain, photoresponse characteristics dominated by the photoconductive effect as well as the photovoltaic effect are investigated. When the device is turned off, it acts as a photoconductor, and by calculating photoconductor gain, the primary photodetected power can be determined, which indicates the absorbed optical power. The ratio between this and the photodetected power due to the photovoltaic effect represents phototransistor internal gain. It is demonstrated that the phototransistor internal gain is function of optical modulation frequency. © *2004 American Institute of Physics.* [DOI: 10.1063/1.1739278]

High-speed field-effect transistors such as metal-semiconductor field-effect transistors (MESFETs) and high-electron-mobility transistors (HEMTs) have been investigated for optical-to-microwave transducer applications.[1] They can provide high internal gain as phototransistors and the possibility of simultaneously performing photodetection and microwave signal processing is quite attractive for such applications as radio-over-fiber systems.[2] Photodection characteristics of high-speed field-effect transistors have been reported by several research groups. Madjar *et al.* reported that there are two photodetection mechanisms, photovoltaic, and photoconductive effects, in GaAs MESFETs.[3] Romero *et al.* presented an analytical model for photodetection in AlGaAs/GaAs HEMTs and explained gate voltage shifts under illumination and their nonlinear dependence on incident optical powers.[4] In addition, they reported that the photovoltaic effect is inherently slow due to long lifetime of photogenerated holes. Takanashi *et al.* showed that the photoconductive effect can be observed at high optical modulation frequencies in backside illuminated InAlAs/InGaAs HEMTs.[5] However, the determination of phototransistor internal gain, although it is an important device performance parameter, has not been reported since the actual absorbed optical power cannot be easily estimated.

In this letter, we demonstrate that the phototransistor internal gain can be determined by estimating the primary photocurrents that are due to absorbed optical power from the device when it acts as a photoconductor. Using metamorphic HEMTs (mHEMTs) grown on a GaAs substrate, we first show that the dominant photodetection mechanism is the photoconductive effect when the device is turned-off, and photovoltaic when turned-on. From the estimation of photocondutor gain when it is turned-off, primary photodetected powers are determined and with these, phototransistor internal gain is determined for optical modulation frequency up to 13.5 GHz.

Epitaxial layer structure of the mHEMT used for our investigation is shown in Fig. 1. This is the same mHEMT structure used for our previous investigation in which large photoresponsivities were reported.[6] InAlAs/InGaAs layers were grown on a semi-insulating GaAs substrate with the help of $In_xAl_{1-x}As$ metamorphic buffer layer which mitigated problems associated with lattice mismatch between substrate and InGaAs channel layers.[7] The mHEMT has $In_{0.53}Ga_{0.47}As/In_{0.35}Ga_{0.65}As$ composite channels in order to enhance high frequency device performance without sacrificing breakdown characteristics.[7] The sheet carrier density and mobility of two-dimensional electron gas (2DEG) are 1.6×10^{12} /cm^2 and 8800 cm^2/V s, respectively at room temperature. The gate length and width of the mHEMT are 0.25 and 50 μm, respectively. The reverse breakdown voltage is -13 V and the maximum transconductance is 520 mS/mm. By measuring *S* parameters of device, the current gain cutoff

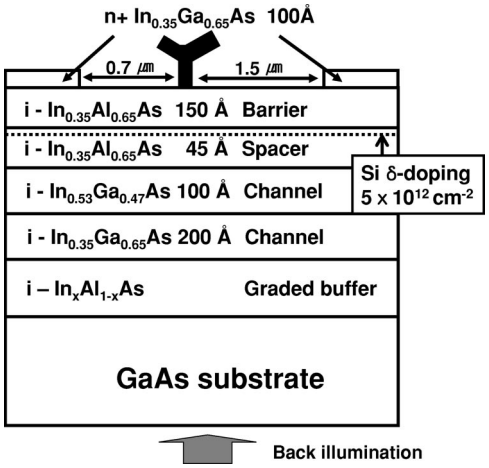

FIG. 1. Epitaxial layer structure of the fabricated mHEMT.

a)Electronic mail: wchoi@yonsei.ac.kr

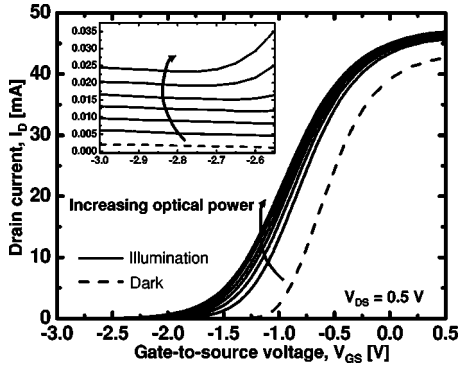

FIG. 2. I_D-V_{GS} characteristic of the mHEMT at $V_{DS}=0.5$ V under dark and illuminated condition. Incident optical power increases from 10 to 60 mW with 10 mW increment, from bottom to top. The inset is enlarged graph at V_{GS} below the threshold voltage, which is turn-off condition.

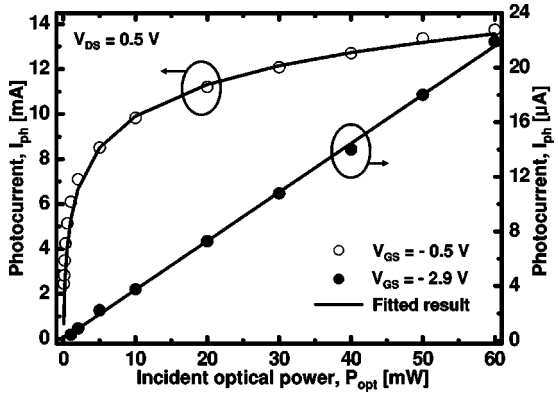

FIG. 3. Photocurrent as a function of incident optical power under turn-on ($V_{GS}=-0.5$ V) and turn-off ($V_{GS}=-2.9$ V) condition at $V_{DS}=0.5$ V. Symbols are measured data and solid lines indicate fitted result using Eqs. (1) and (2).

frequency (f_T) of 60 GHz and maximum oscillation frequency ($f_{\max}$) of 130 GHz are calculated at the drain-to-source voltage (V_{DS}) of 1.5 V and gate-to-source voltage (V_{GS}) of -1.0 V.

To characterize the optical response of the mHEMT, DFB laser diode ($\lambda=1552.5$ nm) was direct modulated and then amplified with erbium-doped fiber amplifier (EDFA) for compensating optical coupling loss. The light injection is done with backside illumination with a lensed fiber, which provided about 10% coupling efficiency. Since 1.55 μm light is transparent to the substrate, buffer layer, and $In_{0.35}Ga_{0.65}As$ channel, optical absorption takes place only in thin 100 Å $In_{0.53}Ga_{0.47}As$ channel layer.

Figure 2 shows I_D-V_{GS} characteristics under dark and illuminated condition with different amounts of incident optical power. When V_{GS} is higher than the threshold voltage (turned-on condition), I_D increases and threshold voltage of the mHEMT shifts negatively with the increasing incident optical power. This is well known to be due to the photovoltaic effect.[6] However, it can be observed that I_D shows small increase as optical power increases when V_{GS} is below the threshold voltage (turned-off condition) as shown in the inset of Fig. 2. This is due to the photoconductive effect in which photogenerated electrons increase the channel conductivity and, consequently, the drain current. This identification for photodetction mechanism can be verified by fitting the measured data to the relationship between photocurrents and incident optical powers due to each mechanism.

The photocurrent caused by the photovoltaic effect can be expressed as[5]

$$I_{ph,pv}=G_M\Delta V_{TH}=\frac{A\cdot kT}{q}\ln\left(1+\frac{\eta q\lambda P_{\text{opt}}}{I_{pd}\cdot hc}\right), \tag{1}$$

where G_M is the transconductance, ΔV_{TH} is the threshold voltage shift, η is the quantum efficiency, P_{opt} is the incident optical power, I_{pd} is the dark current for holes, hc/λ is the photon energy, and A is fitting parameter. The fitted data for turned-on condition in Fig. 3 clearly shows the characteristic logarithmic dependence. At $V_{DS}=0.5$ V and $V_{GS}=-0.5$ V, the fitting parameters, A of 77.6 S and η/I_{pd} of 798.6 A^{-1} in Eq. (1) are obtained.

On the other hand, the photocurrent caused by the photoconductive effect can be described as[8]

$$I_{ph,pc}=(q\mu_n nE)WD=B\cdot P_{\text{opt}}, \tag{2}$$

where μ_n is the electron mobility, n is the electron concentration, E is the electric field in the channel, W is the gate width, D is the depth of absorption region, and B is the fitting parameter. Since the electron concentration is proportional to the incident optical power, Eq. (2) can be derived. The fitted data for turned-off condition show clear linear dependence, confirming that the photoconductive effect is responsible. At $V_{DS}=0.5$ V and $V_{GS}=-2.9$ V, the fitting parameter, B of 0.36 mA/W in Eq. (2) is obtained.

The optical modulation responses were investigated for two different cases under the fixed drain voltage of 1.5 V and the results are shown in Fig. 4. At V_{GS} of -0.5 V (turned-on condition), large photoresponse is obtained due to the internal gain provided by the photovoltaic effect although it decays fast owing to long lifetime of photogenerated holes.[5] In contrast, the optical modulation response at $V_{GS}=-3.5$ V (turned-off condition) is very small but does not fall off as fast since this frequency response is dominated by short electron lifetime.

In order to determine the primary photocurrents, the photoconductor gain should be calculated first, which can be estimated as[8]

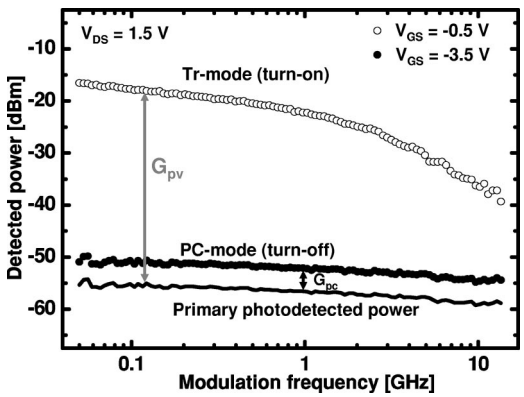

FIG. 4. Optical modulation response of the mHEMT at $V_{GS}=-0.5$ V and $V_{GS}=-3.5$ V under fixed V_{DS} of 1.5 V. The solid line indicates primary photodetected power calculated using photoconductor gain. G_{pc} : photoconductor gain, G_{pv} : phototransistor internal gain provided by the photovoltaic effect, Tr-mode: phototransistor mode, PC-mode: photoconductor mode.

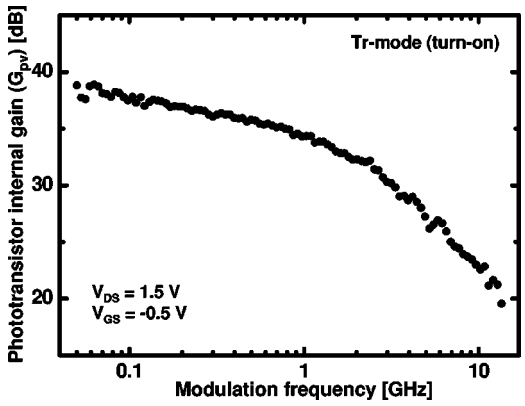

FIG. 5. Phototransistor internal gain (G_{pv}) as a function of optical modulation frequency at $V_{DS}=1.5$ V and $V_{GS}=-0.5$ V.

$$G_{pc}=\frac{I_{ph,pc}}{I_{\text{prime}}}=\frac{\tau_n}{t_n}=\frac{t_p}{t_n}\approx\frac{v_n}{v_p}, \tag{3}$$

where I_{prime} is the primary photocurrent, which represents actual absorbed optical signal in the channel, τ_n is the electron lifetime, t_n is the electron transit time, t_p is the hole transit time, v_p is the hole velocity, and v_n is the electron velocity in the channel. In Eq. (3), electron lifetime can be replaced with hole transit time because electrons are not supplied from the source until holes reach the source region.[9] The ratio of electron and hole transit times can be determined by the ratio of electron to hole saturation velocities in the $In_{0.53}Ga_{0.47}As$ channel[9,10] under identical electric field. As a result, the photoconductor gain of about 1.6 is obtained. With this, the primary photodetected powers can be determined as shown in Fig. 4 and the difference between these and the photodetected powers when the device is turned-on is the phototransistor internal gain. As can be seen in Fig. 5, the metamorphic HEMT exhibits large phototransistor internal gain although it decays rapidly due to the optical modulation response characteristics caused by the photovoltaic effect.

In conclusion, photoreponse characteristics dominated by the photoconductive and photovoltaic effect are investigated and the phototransistor internal gain provided by the photovoltaic effect is determined for mHEMTs. Because photocurrents are only due to the photoconductive effect when the device is turned off, the primary photodetected powers can be estimated with the photoconductor gain. By taking the difference between these and photodetected powers when the device is turned on, phototransistor internal gain is determined. Although our work was done for mHEMTs, a similar approach can be used for other phototransistors based on field-effect transistors.

This work was supported by the Ministry of Science and Technology of Korea through the National Research Laboratory Program.

[1] C. Y. Chen, A. Y. Cho, C. G. Bethea, P. A. Garbinski, Y. M. Pang, B. F. Levine, and K. Ogawa, Appl. Phys. Lett. **42**, 1040 (1983).
[2] A. J. Seeds and A. A. A. De Salles, IEEE Trans. Microwave Theory Tech. **5**, 577 (1990).
[3] A. Madjar, P. R. Herczfeld, and A. Paolella, IEEE Trans. Microwave Theory Tech. **40**, 1681 (1992).
[4] M. A. Romero, M. A. G. Martinez, and P. R. Herczfeld, IEEE Trans. Microwave Theory Tech. **44**, 2279 (1996).
[5] Y. Takanashi, K. Takahata, and Y. Muramoto, IEEE Trans. Electron Devices **46**, 2271 (1999).
[6] C.-S. Choi, H.-S. Kang, W.-Y. Choi, H.-J. Kim, W.-J. Choi, D.-H. Kim, K.-C. Jang, and K.-S. Seo, IEEE Photonics Technol. Lett. **15**, 846 (2003).
[7] M. Chertouk, H. Heiß, D. Xu, S. Kraus, W. Klein, G. Böhm, G. Tränkle, and G. Weimann, *International Conference on Indium Phosphide and Related Material Proceeding*, 1995, p. 737.
[8] S. M. Sze, *Physics of Semiconductor Devices* (Wiley, New York, 1981), p. 744.
[9] K. Brennan, Appl. Phys. Lett. **51**, 995 (1987).
[10] J. L. Thobel, L. Baudry, A. Cappy, P. Bourel, and R. Fauquembergue, Appl. Phys. Lett. **56**, 346 (1989).